Accepted Manuscript



Obesity and spinal loads; a combined MR imaging and subject-specific modeling investigation

M.H. Akhavanfar, H. Kazemi, A.H. Eskandari, N. Arjmand

PII: S0021-9290(17)30419-0
DOI: http://dx.doi.org/10.1016/j.jbiomech.2017.08.009
Reference: BM 8334

To appear in: *Journal of Biomechanics*

Accepted Date: 5 August 2017

Please cite this article as: M.H. Akhavanfar, H. Kazemi, A.H. Eskandari, N. Arjmand, Obesity and spinal loads; a combined MR imaging and subject-specific modeling investigation, *Journal of Biomechanics* (2017), doi: http://dx.doi.org/10.1016/j.jbiomech.2017.08.009

This is a PDF file of an unedited manuscript that has been accepted for publication. As a service to our customers we are providing this early version of the manuscript. The manuscript will undergo copyediting, typesetting, and review of the resulting proof before it is published in its final form. Please note that during the production process errors may be discovered which could affect the content, and all legal disclaimers that apply to the journal pertain.

ACCEPTED MANUSCRIPT

Submitted as Original Article to "Journal of Biomechanics-Berlin Workshop"

(BM-D-17-00407R2)

Obesity and spinal loads; a combined MR imaging and subject-specific modeling investigation

Akhavanfar MH, MSc**, Kazemi H,** MSc**, Eskandari AH,** MSc**, Arjmand N**[*]**,** PhD

Department of Mechanical Engineering, Sharif University of Technology, Tehran, Iran

*** Corresponding Author:**

Navid Arjmand, PhD, Sharif University of Technology

Tehran, 11155-9567, Iran.

Email: **arjmand@sharif.edu**

Word Count (Introduction through Discussion): 4007

Word Count (Abstract): 250

ACCEPTED MANUSCRIPT

ACCEPTED MANUSCRIPT

ABSTRACT

Epidemiological studies have identified obesity as a possible risk factor for low back disorders. Biomechanical models can help test such hypothesis and shed light on the mechanism involved. A novel subject-specific musculoskeletal-modelling approach is introduced to estimate spinal loads during static activities in five healthy obese (BMI>30 kg/m^2) and five normal-weight (20<BMI<25 kg/m^2) individuals. Subjects underwent T1 through S1 MR imaging thereby measuring cross-sectional-area (CSA) and moment arms of trunk muscles together with mass and center of mass (CoM) of T1-L5 segments. MR-based subject-specific models estimated spinal loads using a kinematics/optimization-driven approach. Average CSAs of muscles, moment arms of abdominal muscles, mass and sagittal moment arm of CoM of T1-L5 segments were larger in obese individuals ($p<0.05$ except for the moment arm of CoMs) but moment arms of their back muscles were similar to those of normal-weight individuals ($p>0.05$). Heavier subjects did not necessarily have larger muscle moment arms (e.g., they were larger in 64 kg (BMI=20.7 kg/m^2) subject than 78 kg (BMI=24.6 kg/m^2) subject) or greater T1-L5 trunk weight (e.g., the 97 kg (BMI=31 kg/m^2) subject had similar trunk weight as 109 kg (BMI=33.3 kg/m^2) subject). Obese individuals had in average greater spinal loads than normal-weight ones but heavier subjects did not necessarily have greater spinal loads (117 kg (BMI=40.0 kg/m^2) subject had rather similar L5-S1 compression as 105 kg (BMI=34.7 kg/m^2) subject). Predicted L4-L5 intradiscal pressures for the normal-weight subjects ranged close to the measured values (R^2=0.85-0.92). Obese individuals did not necessarily have greater IDPs than normal-weight ones.

***Keywords*:** Obesity, Spine loads, MR imaging, Musculoskeletal model, Subject-specific.

ACCEPTED MANUSCRIPT

ACCEPTED MANUSCRIPT

Introduction

Obesity is a worldwide growing health challenge affecting up to 30% of the world's population (Haslam and James, 2005). A large population study on ~45,000 working adults indicates associations between higher body mass index (BMI) and musculoskeletal disorders (Viester et al., 2013) including low back pain (LBP) (Nilsen et al., 2011; Shiri et al., 2010). When genetics (familial) factors were controlled this association was however diminished (Dario et al., 2015). It has been therefore suggested that body weight (BW) is a possible weak risk factor for LBP (Leboeuf, 2000) or only probably linked to LBP (Manchikanti, 2000). A recent *in vitro* MR imaging study on intact L4-L5 segments, however, found greater facet degeneration and disc herniation in obese than normal-weight individuals (Rodriguez-Martinez et al., 2016).

Although the obesity-related low back disorders have multifactorial etiology, likely greater mechanical loads on the spine of heavier individuals may play a role. The greater spinal loads in obese individuals is assumingly due to the larger magnitude and anterior moment arms of their upper trunk gravity loads that generate greater flexion moments. However, likely larger trunk extensor muscle moment arms in heavier individuals may partly or fully offset such additional flexion moments. *In vivo* studies have shown that obese individuals experience larger stature loss, as compared to normal-weight ones, during walking (Rodacki et al., 2005) and from supine to upright standing (Yar, 2008); a qualitative indication of larger spinal compressive loads in obese individuals.

In absence of non-invasive *in vivo* approaches, musculoskeletal (MS) models are used to compare spinal loads in obese and normal-weight individuals (Ghezelbash et al., 2016a; Hajihosseinali et al., 2015; Han et al., 2013). These models have used numerical approximations to scale gravity loading, musculature, and/or passive tissue properties with BW and have reported considerably larger spine loads in obese individuals during a number of static activities. For instance, using a linear scaling approach for mass, length and segment-fixed nodes of muscles in AnyBody Modeling System^{TM}, T12-L5 shear and compression loads were found to increase linearly with BW (Han et al., 2013). We used a detailed multi-joint MS model (Hajihosseinali et al., 2014) along with an image-based anisotropic scaling method (Hajihosseinali et al., 2015) to numerically modify musculature with BW. A rather similar

ACCEPTED MANUSCRIPT

image-based scaling approach for muscle parameters was used by Ghezelbash et al. (2016a). They, however, scaled moment arms of gravity loads based on numerical reconstruction of body shape according to available image datasets of human laser scans. Passive joint properties were also numerically scaled with BW based on intervertebral disc height and area (Ghezelbash et al., 2016a). Both latter studies found that BW substantially influenced spinal loads.

These MS models have used population-based datasets, rather than subject-specific ones, to numerically scale muscle parameters and gravity loads with BW. In other words, for a given BW, all model parameters were scaled based on the existing "average" values for the considered BW. As such, they fail to identify the likely differences between spinal loads of individuals with similar BW and BMIs. Moreover, image-based regression equations (Anderson et al., 2012) used in the previous models to scale muscle parameters (Ghezelbash et al., 2016a; Hajihosseinali et al., 2015) are not sensitive, at constant body height (BH), to the cause of increase in BWs, i.e., identical muscle parameters are predicted irrespective of whether BW is increased by gaining fat deposits (as in obese individuals) or by gaining muscle masses (as in athletes). The present study hence aims to:

(1) Use MR images to measure cross-sectional area (CSA), anterior-posterior (AP) and medio-lateral (ML) moment arms (distance from centroid of the corresponding disc) of trunk muscles at all lumbar levels (T12-L5), mass and center of mass (CoM) of all trunk T1-L5 segments, CSAs and height of the lumbar discs (T12-L5) in five healthy abdominal obese (BMI>30 kg/m^2) and five healthy normal-weight (20<BMI<25 kg/m^2) individuals.

(2) Introduce a novel approach to build subject-specific T1-S1 MS models of the ten individuals based on our MR measurements.

(3) Quantify lower lumbar (L4-S1) loads in obese and normal-weight individuals during a number of static activities using the subject-specific MS models.

Materials and Methods

***In vivo* MR measurement study:** A 3.0 Tesla Siemens Trio Tim machine (Erlangen, Germany) was used to obtain transverse images from the supine T1-S1 spine of five healthy young male obese (age: 25.2±1.0 years, BW: 105.2±6.2 kg, BH: 175.4±2.9 cm, BMI = 34.4±2.5 kg/m^2, and

ACCEPTED MANUSCRIPT

maximal waist circumference = 114.0±9.2 cm) and five age-sex-height matched normal-weight (25.0±0.8 years, 70.2±4.6 kg, 175.4±1.5 cm, 22.8±3.8 kg/m^2 and maximal waist circumference = 84.2±4.8 cm) individuals (detailed subjects' characteristics are provided in the Supplementary Data (Excel file)). The institutional ethic committee's approval and informed consent were obtained. The inclusion criteria for the five healthy obese individuals was having a BMI>30 kg/m^2 and maximal waist circumstance≥ 105 cm. T1-weighted images with slice thickness of 5 mm and inter-slice gap of 1 mm were taken starting from the superior endplate of the S1 through slightly above the superior endplate of the T1 vertebra. Subjects laid on the MR table in a relaxed supine position. Identical imaging procedure was followed by the same operator for all subjects.

Images were imported into Mimics® (version 17.0, Materialise, Leuven, Belgium) to measure AP and ML moments arms as well as CSAs of the erector spinae (ES), multifidus (MF), quadratus lumborum (QL), iliopsoas (IP), rectus abdominus (RA), external oblique (EO) and internal oblique (IO) muscles at all lumbar disc levels (T12-L1 through L5-S1), mass and CoM of all T1-L5 segments and CSAs and mid-height of the T12-L5 discs (Figure 1a). The procedure to measure muscle parameters from MR images is described in our recent work (Ghiasi et al., 2016). In brief, outer fascial boundaries of each muscle were traced using a mouse-guided tool while excluding extra-muscular fat and connective tissues (Figure 1b). The software calculated the encompassed area within the traced boundary of each muscle as well as the centroid of this area. Intramuscular non-contractile (fat and connective tissues) components of muscles were identified by analyzing signal intensity of pixels. CSAs of contractile (pure muscle) components as well as AP and ML distance of muscle centroid to disc centroid at all lumbar disc levels (T12-L1 through L5-S1), were subsequently calculated by the software. Note that these AP and ML distances are transverse (not orthogonal) distances obtained directly from the MR images.

Mass and center of mass (CoM) of the head and arms (which are not seen in the MR images) were considered based on the available anthropometric data (8.23% and 5.33% of the BW for the head and each arm, respectively) (Plagenhoef et al., 1983). Mass and CoM of the trunk were measured for the T1 to L5 segments based on the MR images. To do this, pixel regions at bones, muscles, adipose sites, visceral organs, and lung tissues were sampled from MR images (Pearsall et al., 1994 and 1996). Density values were assigned to the bones (1.5 g/cc), muscles (1.06 g/cc),

ACCEPTED MANUSCRIPT

adipose sites (0.96 g/cc), visceral tissues (1.06 g/cc), and lung tissues (0.25 g/cc) (Pearsall et al., 1994 and 1996). Position of CoM and weight at each segment (i.e., between mid-heights of adjacent discs) were subsequently estimated using an in-house code.

Reference subject: To build an accurate reference MS model based on which MS models of the other ten subjects are scaled (see below), an additional normal-weight asymptomatic young male subject (170 cm, 64 kg, BMI = 22.1 kg/m^2, and 28 years) was volunteered for CT and MR imaging sessions. In the supine posture with fully extended legs, CT images of the sacrum to T11 were taken. To avoid excessive radiation to the subject, his thoracic geometry was constructed using the same 3.0-T MR scanner. Individual vertebrae and pelvis were segmented by a combination of thresholding and manual segmentation to create 3D vertebral models as described in our recent study (Eskandari et al., 2017).

Subject-specific MS model for the reference subject: Details on building the subject-specific (for musculature, geometry, mass, and center of masses) T1-S1 MS trunk model for the reference subject are provided elsewhere (Eskandari et al., 2017). In brief, to construct spine profile in the supine posture, CT and MRI images in the mid-sagittal plane of the spine were selected. From these images, the bony anatomy of each vertebra and then its geometric centroid were estimated in Mimics® (version 17.0). The thoracic spine profile (constructed based on MR images) was added to the lumbar profile (constructed from CT images) (Figure 2a). CSA of each lumbar disc was digitally determined at its mid-height plane. Muscle parameters as well as trunk mass and CoMs were determined from the MR and CT images using the same procedure explained earlier (Figure 2b).

A sagittally-symmetric subject-specific architecture for trunk muscles was developed for the reference subject using the upper and lower insertion sites of muscles determined based on CT and MR images (Bogduk et al., 1992; Stokes and Gardner-Morse, 1999) (Figure 2c). 46 bilateral local muscles attached to lumbar vertebrae and 10 bilateral global muscles attached to the thoracic spine were included in the model. While total CASs of muscles were considered based on our CT and MR measurements, those of individual muscle fascicles were determined based on data reported in the literature (Stokes and Gardner-Morse, 1999). The T12-S1 intervertebral

ACCEPTED MANUSCRIPT

discs were modeled by 6 shear-deformable beams with nonlinear load-displacement curves under axial/shear forces and sagittal/lateral/axial moments (Figure 2c) that were taken identical for all subjects (Shirazi-Adl, 2006).

Subject-specific MS models for other subjects: For each individual, a subject-specific T1-S1 MS model was developed by scaling the reference model (Figure 3). To do this, for each subject, average changes in the measured CSAs and moment arms of muscles at T12-S1 levels with respect to those measured for the reference subject were calculated and the MS model was scaled accordingly. For instance, if the measured AP moment arm of a given muscle for the subject under consideration was 30% larger than that of the reference subject, the muscle was moved posteriorly so as to have 30% larger moment arm in the model. Mass and CoM of the upper trunk was also considered for each subject based on the MR measurements described earlier.

Simulated tasks: Various static symmetric activities in upright and flexed postures were simulated using the developed MS models (Figure 4). Required kinematics (trunk and pelvis orientations as well as position of arms and hand load for each task) were taken from our previous motion analysis on a healthy male subject (52 years, 174.5 cm and 68.4 kg) (Arjmand et al., 2009 and 2010).

Calculation of muscle forces and spinal loads: The supine posture was assumed as the unloaded posture with no initial muscle forces and spinal loads. The upright standing posture with no load in hands was estimated for each subject based on an optimization approach that minimizes muscle activities in upright standing (El-Rich et al., 2004; Shirazi-Adl et al., 2002). As subjects had different musculatures, body weights, and segmental CoMs, the optimization algorithm estimated 11 different relaxed upright postures for the subjects (subject-specific upright postures). Subsequently, for each task, the pelvis and thorax kinematics (rotations) acquired from our previous motion analysis under the forgoing tasks (Arjmand et al., 2009 and 2010) were prescribed into the model in the upright posture to reconstruct kinematics of the spine. As for the individual lumbar vertebrae, the total lumbar rotation, calculated as the difference between the T12 and S1 rotations, was partitioned in accordance with constant proportions reported in earlier investigations (Bazrgari et al., 2008). Our previously developed

ACCEPTED MANUSCRIPT

and validated kinematics- and optimization-driven approach (cost function of minimum sum of cubed muscle stresses) was used to calculate muscle forces and spine loads under the foregoing static activities (Arjmand and Shirazi-Adl 2006a, b, and c).

Model validation: Predictions of the MS models for L4-L5 intradiscal pressure (IDP) were compared with available *in vivo* IDPs (Wilke et al., 2001) for a numebr of static activities (see below). A quadratic regression equation (Ghezelbash et al., 2016a) was used to estimate IDP based on the axial compression force and intersegmental flexion rotation for each activity.

Statistical analysis: Unpaired (two sample) t-tests (to determine if two sets of data are significantly different from each other) were conducted to compare the mean of each measured or predicted parameter in the obese individuals to the mean of the corresponding parameter in the normal-weight individuals.

Results

***In vivo study*:** Subject-specific data for T12-L5 CSA of muscles, their AP and ML moment arms, lumbar lordosis and thoracic kyphosis angles, T1-L5 segmental masses and their CoMs relative to the corresponding vertebrae, as well as T12-L5 disc CSAs and mid-heights are reported in Supplementary Data (Excel file). Average CSAs of all muscles were larger in obese individuals as compared to normal-weight ones ($p<0.05$ except for RA, IO, and IP) (Figure 5a). AP moment arms of abdominal muscles (RA, EO, IO) were significantly larger in obese individuals ($p<0.05$) at all lumbar T12-L5 levels while those of their back muscles (ES, MF, and QL) were almost equal to those of normal-weight ones ($p>0.05$) (Figure 5b). Subject-specific analysis of results indicated that subjects with greater BWs did not necessarily have greater muscle moment arms (Supplementary Data). For instance, the subject with BW = 64 kg (BMI = 20.7 kg/m^2) had greater AP moment arms for the ES muscle (at all levels) as compared to the subject with BW = 78 kg (BMI = 24.6 kg/m^2).

Mass of all T1-L5 segments was significantly larger (e.g., by ~75% at the L1-L5 levels) in obese individuals ($p<0.05$) (Figure 6a). AP moment arm of CoMs of T1-L5 segments were larger in obese individuals (up to 1.5 cm at some levels) but with no statistical significance in most

ACCEPTED MANUSCRIPT

segments (Figure 6b). This was despite the fact that mean waist circumference of obese individuals was significantly larger than that of normal subjects by ~30 cm. T12-L5 disc CSAs were larger in obese individuals by <10% in average ($p>0.05$) (Figure 7a). For obese individuals, disc mid-heights were slightly larger at the T12-L3 ($p>0.05$) and smaller at the L3-L5 ($p>0.05$) (Figure 7b). Subject-specific analysis of results indicated that subjects with greater BWs and BMIs did not necessarily have greater T1-L5 trunk weight. For instance, the subjects with BW = 97 kg (BMI = 31 kg/m^2) and 109 kg (BMI = 33.3 kg/m^2) had similar upper trunk masses (~33 kg) while the subject with BW = 98 (BMI = 32.4 kg/m^2) kg had smaller upper trunk mass (by ~4.5 kg) than the subject with BW = 97 kg (Supplementary Data).

***Model study*:** For all the simulated activities, average compressive and shear loads on the L5-S1 and L4-L5 discs were larger in obese individuals as compared to normal-weight subjects (Figure 8) ($p<0.05$ except for the two lifting tasks in upright posture). Subject-specific analysis of results, however, indicated (Figure 9) that for a given activity subjects with similar BWs and BMIs did not necessarily experience identical loads on their spines (e.g., compare spinal loads for the two subjects with BWs of 72 kg or 64 kg in the normal-weight group). Moreover, subjects with greater BW and BMI did not necessarily experience greater spinal loads under identical activities. For instance, the subject with BW = 117 kg (BMI = 40.0 kg/m^2) had rather similar L5-S1 compression as the subject with BW = 105 kg (BMI = 34.7 kg/m^2) but considerably larger spinal loads than the subject with BW = 109 kg (BMI = 33.3 kg/m^2). Also, the subject with BW = 109 kg (BMI = 33.3 kg/m^2) had similar spinal compression as the subject with 98 kg (BMI = 32.4 kg/m^2) and the subject with BW = 78 kg (BMI = 24.6 kg/m^2) had similar spinal loads as the subject with BW = 72 kg (BMI = 23.5 kg/m^2).

Inter- and intra-group (normal-weight versus obese) differences for spinal loads were more pronounced at larger trunk flexion angles (Figures 8 and 9). For the two lifting (19.8 kg) tasks in upright posture some of the normal-weight subjects had greater spinal loads than some of obese individuals (for instance, the reference subject with BW = 64 kg had greater L5-S1 compression than the subject with BW = 109 kg) (Figure 9). Predicted L4-L5 IDPs for the normal-weight subjects ranged close to the measured IDPs in a normal-weight subject (BW $\cong$ 70 kg) (Wilke et al., 2001) for all activities (correlation coefficients, R^2, ranged from 0.85 to 0.92) except in the

ACCEPTED MANUSCRIPT

loaded activities in which the predicted IDPs were larger than the measured values (Figure 10). Obese individuals did not necessarily have greater IDPs than normal-weight ones.

Discussion

Effect of obesity on the spinal loads was investigated using subject-specific MS models. Although obese individuals had in average greater spinal loads than normal-weight ones but subjects with greater BW did not necessarily have greater spinal loads. Spinal loads depend on upper trunk BW, trunk CoMs and musculature that can be totally different between two subjects with identical BWs and BMIs. Results of the population-based models should hence be interpreted with caution.

Analysis of Results: In agreement with the previous population-based modeling investigations (Ghezelbash et al., 2016b; Hajihosseinali et al., 2015; Han et al., 2013), our results indicate that obese individuals experience greater average spinal loads than normal-weight ones under a given activity (Figure 8). Obesity should therefore be considered as a biomechanical risk factor for LBP. At a constant BW, population-based models consider identical trunk mass, trunk CoMs, and musculature in the MS model and thus predict identical spinal loads regardless of how BW is distributed along the spine. Results of our *in vivo* study, however, clearly indicates that at a constant BW, muscle parameters (moment arms and CSAs), trunk mass and CoMs can be different (Supplementary Data). Moreover, although obese individuals had significantly larger muscle CSAs, abdominal muscle moment arms, and trunk masses but due to the considerable amount of posterior fat (Figure 1b) they did not have larger moment arms for back muscle and trunk CoMs. Consequently, our subject-specific models did not necessarily predict larger spinal loads in heavier individuals or similar spinal loads in subjects with similar BW and BMIs (Figure 9).

In agreement with our previous population-based model study (Hajihosseinali et al., 2015), for the two tasks in upright posture with 19.8 kg in hands, the upper trunk shifted posteriorly (i.e., backward extension of the trunk) (Figure 4) thus moving the center of mass of the upper trunk

ACCEPTED MANUSCRIPT

posteriorly to the L5-S1. This helps exploit the extension moment of the gravity to counterbalance the large flexion moment of the external load held in hands. This auxiliary extension moment that were larger in obese individuals reduced extensor muscle forces and thus spinal loads in some obese individuals as compared to normal-weight ones (Figure 9).

Predicted IDP for a given activity was in some cases smaller in obese individuals as compared to the normal-weight ones (e.g., the subject with BW = 109 kg had smaller IDPs in all tasks as compared to the subject with BW = 98 kg) (Figure 10). This is because magnitude of the IDP greatly depends on not only disc compression but also the disc CSA that is very different between subjects. The subject with BW = 98 kg (disc CSA = 1187 mm^2) had smaller disc compression but greater IDP as compared to the subject with BW = 105 kg (disc CSA = 1900 mm^2). When comparing predictions with *in vivo* data, one should note that *in vivo* IDPs were collected in only one subject (Wilke et al., 2001) thus neglecting inter-individual variabilities. Moreover, the regression equation used to estimate the IDP in the MS model (Ghezelbash et al., 2016a) is only suitable for sagittally symmetric tasks involving flexion intersegmental rotations that may affect the estimated IDPs for the two loaded tasks that involve trunk extension.

Limitations: Musculature of the models was scaled using our MR images in which detailed muscle fascicles cannot be seen. Total CSAs and moment arms of major trunk muscles (ES, MF, QL, IP, RA, EO, and IO) were therefore used to develop the MS models (Eskandari et al., 2017). As such, moment arms of all MF fascicles, for instance, that are attached to different L1-L5 lumbar vertebrae were scaled based on the MR images obtained for the bulk of this muscle at different levels. In order to estimate segmental masses from MR images, some constant densities were assumed for different tissues from the literature (Pearsall et al., 1994 and 1996). Apart from different density values that have been reported in the literature (Matrangola et al., 2008), the density may also vary within a given tissue, e.g., from 1.1 to 1.8 g/cc for cancellous and cortical bone, respectively (Pearsall et al., 1994). This could have influenced our estimated segmental masses and CoMs. Our analyses, however, show that only ~6-10% (depending on the subject and spinal level) of segmental masses is generated by vertebral masses. Inter-rater reliability in identifying outer facial boundaries of muscles was not investigated in the present study. Using

ACCEPTED MANUSCRIPT

the same MR machine and procedure to identify muscle borders, we assessed and confirmed inter-rater agreement in our previous study (Ghiasi et al., 2016).

We only scaled trunk mass, its CoMs, and musculature of the MS models based on the MR images while passive properties of the joints were taken identical for all subjects regardless of their BW. This was due to lack of a non-invasive *in vivo* approach to measure subject-specific passive stiffness. A recent *in vitro* study on 168 intact L4-L5 spinal segments revealed no significant differences in range of motion of obese and non-obese donors during flexion-extension or lateral bending loading (Rodriguez-Martinez et al., 2016). This, along with non-significant differences between disc CSA and height of obese and normal-weight subjects of the present study (Figure 7), may together indicate that obesity has negligible effect on the passive stiffness of the spinal joints. While the initial spinal shape (including lumbar lordosis and thoracic kyphosis) in the supine posture was not individualized in the model, the relaxed upright spinal shape of each subject was estimated based on the described optimization approach that minimizes muscle activities in upright standing (El-Rich et al., 2004; Shirazi-Adl et al., 2002). Sensitivity analyses show that variations in the lumbar lordosis can affect spinal loads (Ghezelbash et al., 2017). For instance, increasing lumbar lordosis by 10º reduced the L5-S1 compression and increased L5-S1 shear forces by 12 and 29%, respectively (Ghezelbash et al., 2017). Initial line of action of muscles were taken identical to those measured from the CT images of the reference subject. This was because transverse MR images do not provide accurate information on the bony insertions of muscles that are needed to estimate their lines of action. Such an assumption can influence our model predictions as lines of action and thus orthogonal moment arms of muscles can be different from one subject to another especially from normal to obese individuals.

For the simulated tasks in a given trunk flexion angle, identical pelvis and lumbar vertebral rotations were considered in all subjects. Note that subject-specific models, however, had slightly different postures under a given activity as trunk, pelvis, and vertebral rotations were prescribed onto the subject-specific models of the relaxed upright postures. While subject- and task-specific pelvis rotations can be measured via a common skin-based motion analysis, those of the vertebrae can be measured via an upright imaging technique (Eskandari et al., 2017). This

ACCEPTED MANUSCRIPT

shortcoming may become crucial in simulation of tasks in upright posture with load in hands. This is because while posterior shift of the upper trunk during anterior load handling of 20 kg was observed and measured in our *in vivo* study on one healthy individual (Arjmand et al., 2009) as well as in the study of Wilke et al., 2001, this may not be generalized to all subjects with different arm strength, magnitude of hand load, and body weights. The optimization-driven approach used to predict muscle forces and thus spinal loads fails to assign any force to antagonistic muscles and naturally had a deterministic nature, i.e., inter-individual variabilities in load-sharing among muscles cannot be predicted.

ACCEPTED MANUSCRIPT

ACCEPTED MANUSCRIPT

Acknowledgment

This work was supported by grants from the Iran National Science Foundation (INSF) (grant number: 95815353) and Sharif University of Technology (Tehran, Iran). Assistance of Prof. M. Parnianpour and Prof. A. Shirazi-Adl in both modelling procedure and processing of MR images as well as Mr. F. Ghezelbash in performing statistical analyses is greatly appreciated.

Conflict of interest statement

The authors have no conflicts of interest concern.

ACCEPTED MANUSCRIPT

ACCEPTED MANUSCRIPT

References

Anderson, D.E., D'Agostino, J.M., Bruno, A.G., Manoharan, R.K., Bouxsein, M.L., 2012. Regressions for estimating muscle parameters in the thoracic and lumbar trunk for use in musculoskeletal modeling. Journal of Biomechanics 45, 66-75.

Arjmand, N., Shirazi-Adl, A., 2006a. Sensitivity of kinematics-based model predictions to optimization criteria in static lifting tasks. Med. Eng. Phys. 28, 504-514.

Arjmand, N., Shirazi-Adl, A., 2006b. Model and in vivo studies on human trunk load partitioning and stability in isometric forward flexions. Journal of Biomechanics 39, 510-521.

Arjmand, N., Shirazi-Adl, A., 2006c. Role of intra-abdominal pressure in the unloading and stabilization of the human spine during static lifting tasks. European Spine Journal 15, 1265-1275.

Arjmand, N., Shirazi-Adl, A., Bazrgari, B., 2006. Wrapping of trunk thoracic extensor muscles influences muscle forces and spinal loads in lifting tasks. Clinical biomechanics 21, 668-675.

Arjmand, N., Gagnon, D., Plamondon, A., Shirazi-Adl, A., Larivière, C., 2009. Comparison of trunk muscle forces and spinal loads estimated by two biomechanical models. Clinical Biomechanics 24, 533-41.

Arjmand, N., Gagnon, D., Plamondon, A., Shirazi-Adl, A., Larivière, C., 2010. A comparative study of two trunk biomechanical models under symmetric and asymmetric loadings. Journal of Biomechanics 43, 485-91.

Bazrgari, B., Shirazi-Adl, A., Trottier, M., Mathieu, P., 2008. Computation of trunk equilibrium and stability in free flexion–extension movements at different velocities. Journal of biomechanics 41, 412-421.

Bogduk, N., Macintosh, J.E., Pearcy, M.J., 1992. A universal model of the lumbar back muscles in the upright position. Spine 17, 897-913.

Dario, A.B., Ferreira, M.L., Refshauge, K.M., Lima, T.S., Ordoñana, J.R., Ferreira, P.H., 2015. The relationship between obesity, low back pain, and lumbar disc degeneration when genetics and the environment are considered: a systematic review of twin studies. Spine J. 15, 1106-17.

El-Rich, M., Shirazi-Adl, A., Arjmand, N., 2004. Muscle activity, internal loads, and stability of the human spine in standing postures: Combined model and in vivo studies. Spine 29, 2633-42.

Eskandari, A.H., Arjmand, N., Shirazi-Adl, A., Farahmand, F., 2017. Subject-specific 2D/3D image registration and kinematics-driven musculoskeletal model of the spine. Journal of Biomechanics 57, 18-26. doi: 10.1016/j.jbiomech.2017.03.011.

Ghezelbash, F., Shirazi-Adl, A., Arjmand, N., El-Ouaaid, Z., Plamondon, A., 2016**a**. Subject-specific biomechanics of trunk: musculoskeletal scaling, internal loads and intradiscal pressure estimation. Biomech Model Mechanobiol. 15, 1699-1712.

ACCEPTED MANUSCRIPT

Ghezelbash, F., Shirazi-Adl, A., Arjmand, N., El-Ouaaid, Z., Plamondon, A., Meakin, J.R., 2016b. Effects of sex, age, body height and body weight on spinal loads: Sensitivity analyses in a subject-specific trunk musculoskeletal model. Journal of Biomechanics 49, 3492-3501.

Ghezelbash, F., Shirazi-Adl, A., Plamondon, A., Arjmand, N., Parnianpour, M., 2017. Obesity and Obesity Shape Markedly Influence Spine Biomechanics: A Subject-Specific Risk Assessment Model. Ann Biomed Eng. Jun 12. doi: 10.1007/s10439-017-1868-7.

Ghiasi, M.S., Arjmand, N., Shirazi-Adl, A., Farahmand, F., Hashemi, H., Bagheri, S., Valizadeh, M., 2016. Cross-Sectional Area of Human Trunk Paraspinal Muscles before and after Posterior Lumbar Surgery using Magnetic Resonance Imaging. Eur Spine J. 25, 774-82.

Hajihosseinali, M., Arjmand, N., Shirazi-Adl, A., Farahmand, F., Ghiasi, M., 2014. A novel stability and kinematics-driven trunk biomechanical model to estimate muscle and spinal forces. Medical engineering & physics 36, 1296-1304.

Hajihosseinali, M., Arjmand, N., Shirazi-Adl, A., 2015. Effect of body weight on spinal loads in various activities: A personalized biomechanical modeling approach. Journal of Biomechanics 48, 276-282.

Han, K.S., Rohlmann, A., Zander, T., Taylor, W.R., 2013. Lumbar spinal loads vary with body height and weight. Medical Engineering & Physics 35, 969-77.

Haslam, D.W., James, W.P., 2005. Obesity. Lancet 366:1197-209.

Leboeuf-Yde, C., 2000. Body weight and low back pain. A systematic literature review of 56 journal articles reporting on 65 epidemiologic studies. Spine 25, 226-37.

Manchikanti, L., 2000. Epidemiology of low back pain. Pain Physician 3,167-92.

Matrangola, S.L., Madigan, M.L., Nussbaum, M.A., Ross, R., Davy, K.P., 2008. Changes in body segment inertial parameters of obese individuals with weight loss. Journal of Biomechanics 41, 3278-3281.

Nilsen, TI., Holtermann, A., Mork, P.J., 2011. Physical exercise, body mass index, and risk of chronic pain in the low back and neck/shoulders: longitudinal data from the Nord-Trondelag Health Study. Am J Epidemiol. 174, 267-73.

Pearsall, D.J., Reid, J.G., Ross, R., 1994. Inertial properties of the human trunk of males determined from magnetic resonance imaging. Ann Biomed Eng. 22, 692-706.

Pearsall, D.J., Reid, J.G., Livingston, L.A., 1996. Segmental inertial parameters of the human trunk as determined from computed tomography. ANN. BIOMED. ENG. 24, 198-210.

Plagenhoef, S., Evans, F.G., Abdelnour, T., 1983. Anatomical data for analyzing human motion. Resarch Quarterly for Exercise and Sport 54, 169-178.

Rodacki, A.L., Fowler, N.E., Provensi, C.L., Rodacki, Cde L., Dezan, V.H., 2005. Body mass as a factor in stature change. Clinical Biomechanics 20, 799-805.

ACCEPTED MANUSCRIPT

Rodriguez-Martinez, N.G., Perez-Orribo, L., Kalb, S., Reyes, P.M., Newcomb, A.G., Hughes, J., Theodore, N., Crawford, N.R., 2015. The role of obesity in the biomechanics and radiological changes of the spine: an in vitro study. J Neurosurg Spine 24, 615-23.

Shirazi-Adl, A., 2006. Analysis of large compression loads on lumbar spine in flexion and in torsion using a novel wrapping element. Journal of Biomechanics 39, 267-275.

Shirazi-Adl, A., Sadouk, S., Parnianpour, M., Pop, D., El-Rich, M., 2002. Muscle force evaluation and the role of posture in human lumbar spine under compression. European Spine Journal 11, 519-26.

Shiri, R., Karppinen, J., Leino-Arjas, P., Solovieva, S., Viikari-Juntura, E., 2010. The association between obesity and low back pain: a meta-analysis. Am J Epidemiol. 171, 135-54.

Stokes, I.A., Gardner-Morse, M., 1999. Quantitative anatomy of the lumbar musculature. Journal of biomechanics 32, 311-316.

Wilke, H.-J., Neef, P., Hinz, B., Seidel, H., Claes, L., 2001. Intradiscal pressure together with anthropometric data–a data set for the validation of models. Clinical Biomechanics 16, S111-S126.

Yar, T., 2008. Spinal shrinkage as a measure of spinal loading in male Saudi university students and its relationship with body mass index. Saudi Medical Journal 29, 1453-7.

ACCEPTED MANUSCRIPT

ACCEPTED MANUSCRIPT

Figure Captions

Figure 1: MR images at the L4-L5 disc for one typical normal-weight (a) and obese (b) individual (top). Digitizing muscles through their fascial boundaries using a mouse-guided tool to measure their cross-sectional areas (CSAs) at the L4-L5 level in Mimics® (bottom). While the multifidus muscle was carefully isolated, using the fascial border, separating it from the more laterally located longissimus, no attempt was made to separate longissimus and iliocostalis muscles as their boundary was unclear in most of the images; they were considered as one muscle (ES). For the same reason, IO and transverse abdominus muscles were not separated.

Figure 2: (a) Construction of the reference subject's spine geometry using CT and MR images in the supine posture. (b) Position of segmental center of masses (CoMs) relative to the corresponding vertebral body centroids. (c) Individualized spine muscle architecture for the reference subject in the supine posture in sagittal (left) and frontal (right) planes. Local muscles: ICPL: iliocostalis lumborum pars lumborum, LGPL: longissimus thoracis pars lumborum, MF: multifidus, QL: quadratus lumborum, and IP: iliopsoas. Global back muscles: ICPT: iliocostalis lumborum pars thoracic and LGPT: longissimus thoracis pars thoracic. Global abdominal muscles: IO: internal oblique, EO: external oblique, and RA: rectus abdominus. To simulate curved paths of global extensor muscles in flexed postures (i.e., ICPT and LGPT), they were restrained, if necessary, to wrap around predefined vertebral points in between their insertions while incorporating the forces generated at wrapping contact points as additional external loads on the spine (Arjmand et al., 2006).

Figure 3: Ten subject-specific musculoskeletal (MS) models for normal-weight (top) and obese (bottom) individuals in the frontal (a) and sagittal (b) planes. In all models, line of action of muscles were taken identical to that of the reference model (only moment arms and CSAs of muscles were scaled).

Figure 4: Schematics of the simulated tasks to predict spinal loads in different upright and flexed postures without (top) and with (bottom) hand load. This included the relaxed upright standing, forward upper trunk flexion of 10, 20, 30, 40, 50, 60, 70, 80, 90, and 100º with arms in the gravity direction, holding a weight of 19.8 kg close to and away from the chest in the upright posture.

Figure 5: (a) Average cross-sectional area (CSA) of different muscles at T12-S1 levels. (b) Average anterior-posterior (AP) moment arm of different muscles at the L4 level. Standard deviation values as well as statistical significance (between normal-weight and obese individuals at $p < 0.05$*) are also shown on the chart bars. RA: rectus abdominus, EO: external oblique, IO: internal oblique, ES: erector spinae, MF: multifidus, QL: quadratus lumborum, and IP: iliopsoas (R and L denote muscles on the right and left side, respectively).

Figure 6: (a) Segmental mass (kg) at different T1-L5 levels. (b) Anterior-posterior (AP) moment arm of center of mass (CoM) at different T1-L5 levels. Standard deviation values as well as statistical significance (between normal-weight and obese individuals at $p < 0.05$*) are also shown on the chart bars.

ACCEPTED MANUSCRIPT

Figure 7: Disc cross-sectional area (CSA) (a) and disc mid-height (b) at different levels. Standard deviation values are also shown on the chart bars. No statistical significance was observed between obese and normal-weight subjects.

Figure 8: average (and standard deviation) L5-S1 compression (a) and posterior-anterior shear (b) forces for the normal-weight and obese individuals in different activities. Statistical significance (between normal-weight and obese individuals at $p < 0.05$*) are also shown on the chart bars. Results are not provided for the L4-L5 disc as trends were similar to the predicted L5-S1 loads.

Figure 9: Subject-specific L5-S1 compression (a) and posterior-anterior shear (b) forces for normal-weight and obese individuals in different activities. Body weight (BW) and body mass index (BMI) of each subject are provided. Two of the normal-weight models could not simulate the activity with 19.8 held far from body as their back muscles became saturated.

Figure 10: Measured (Wilke et al., 2001) and predicted L4-L5 intradiscal pressure (IDP) values for normal-weight and obese individuals in different activities. Body weight (BW) and L4-L5 disc cross sectional area of each subject are provided. *In vivo* values for flexion angles of 50 to 90° were estimated using interpolation from data provided by Wilke et al., 2001.

ACCEPTED MANUSCRIPT

ACCEPTED MANUSCRIPT

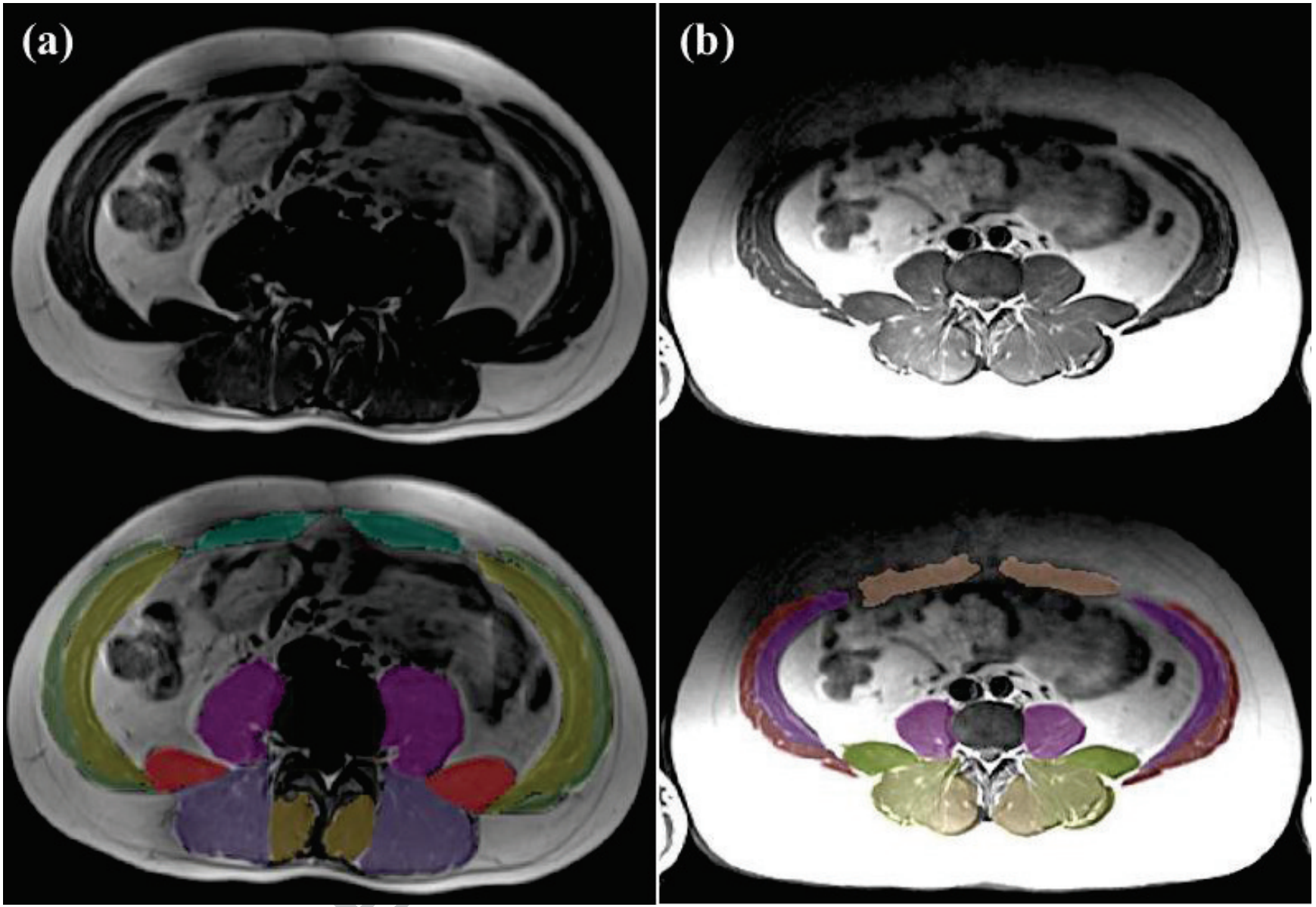
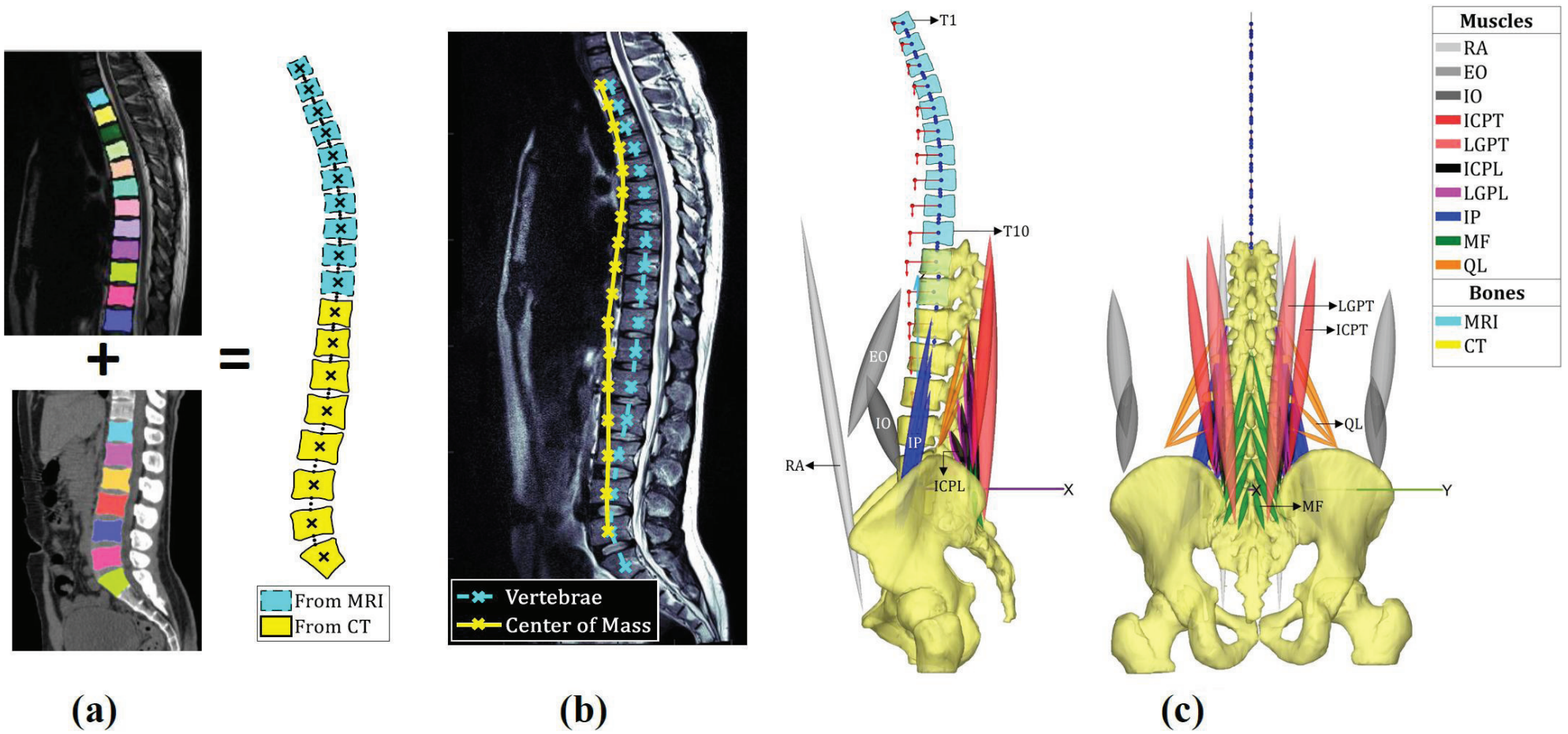


Figure 1


From MRI
From CT
Vertebrae
Center of Mass
T1
T10
EO
IO
IP
RA
ICPL
X
LGPT
ICPT
QL
MF
Y
Muscles
RA
EO
IO
ICPT
LGPT
ICPL
LGPL
IP
MF
QL
Bones
MRI
CT

(a) (b) (c)

ACCEPTE

ACCEPTED MANUSCRIPT

Figure 2

ACCEPTED MANUSCRIPT

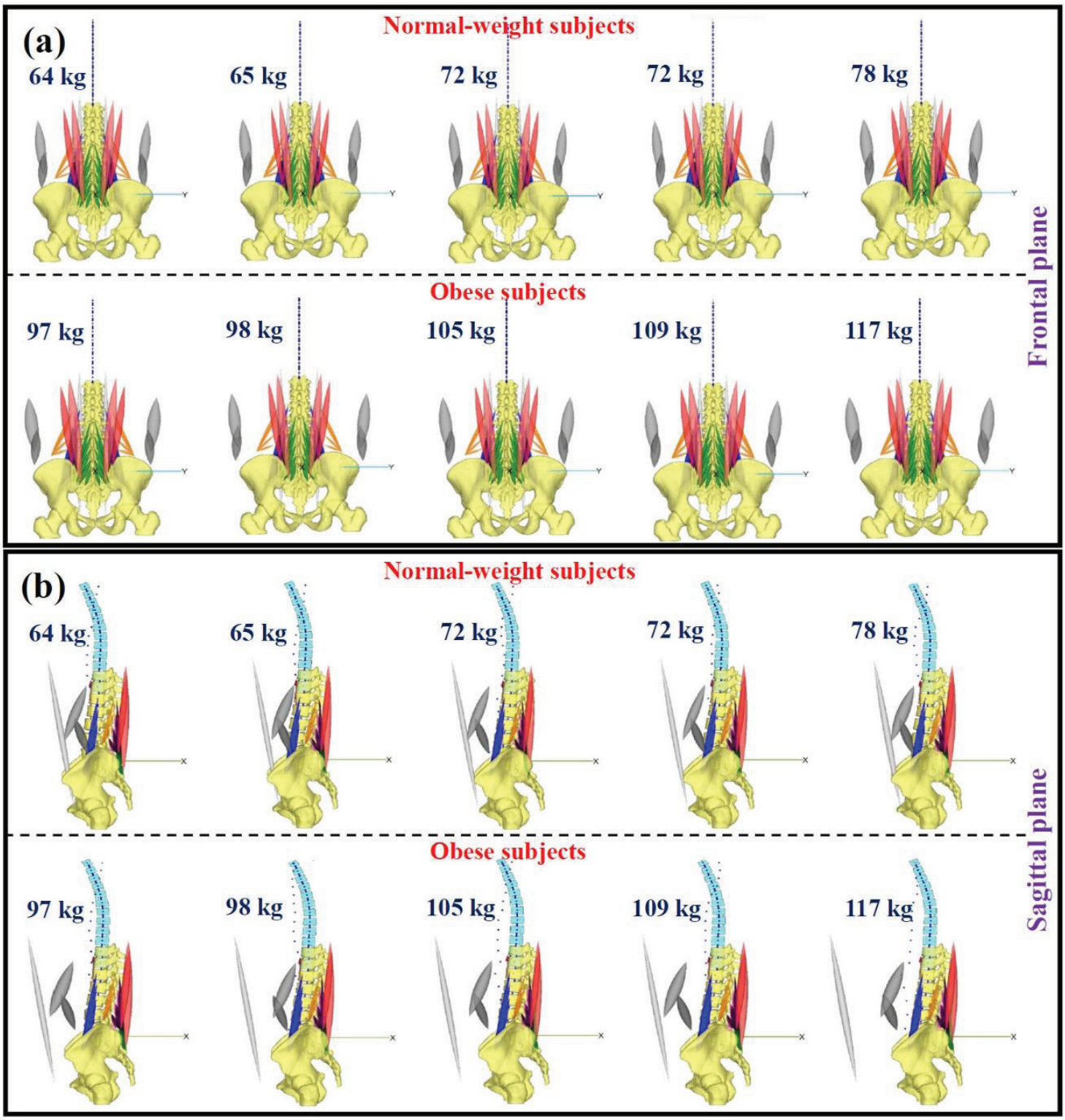

(a)
Normal-weight subjects
64 kg
65 kg
72 kg
72 kg
78 kg
Obese subjects
97 kg
98 kg
105 kg
109 kg
117 kg
Frontal plane
(b)
Normal-weight subjects
64 kg
65 kg
72 kg
72 kg
78 kg
Obese subjects
97 kg
98 kg
105 kg
109 kg
117 kg
Sagittal plane

Figure 3

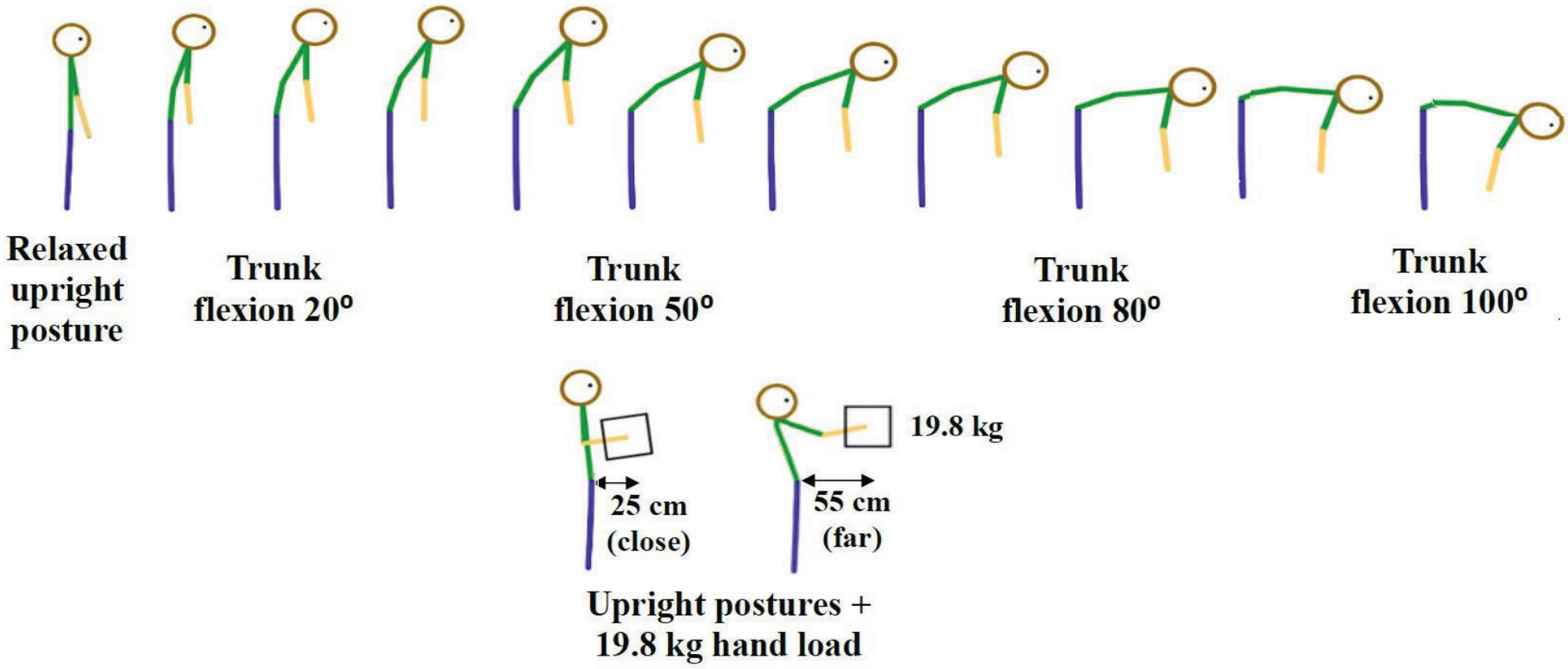

Relaxed upright posture
Trunk flexion 20°
Trunk flexion 50°
Trunk flexion 80°
Trunk flexion 100°
25 cm (close)
55 cm (far)
19.8 kg
Upright postures + 19.8 kg hand load

Figure 4

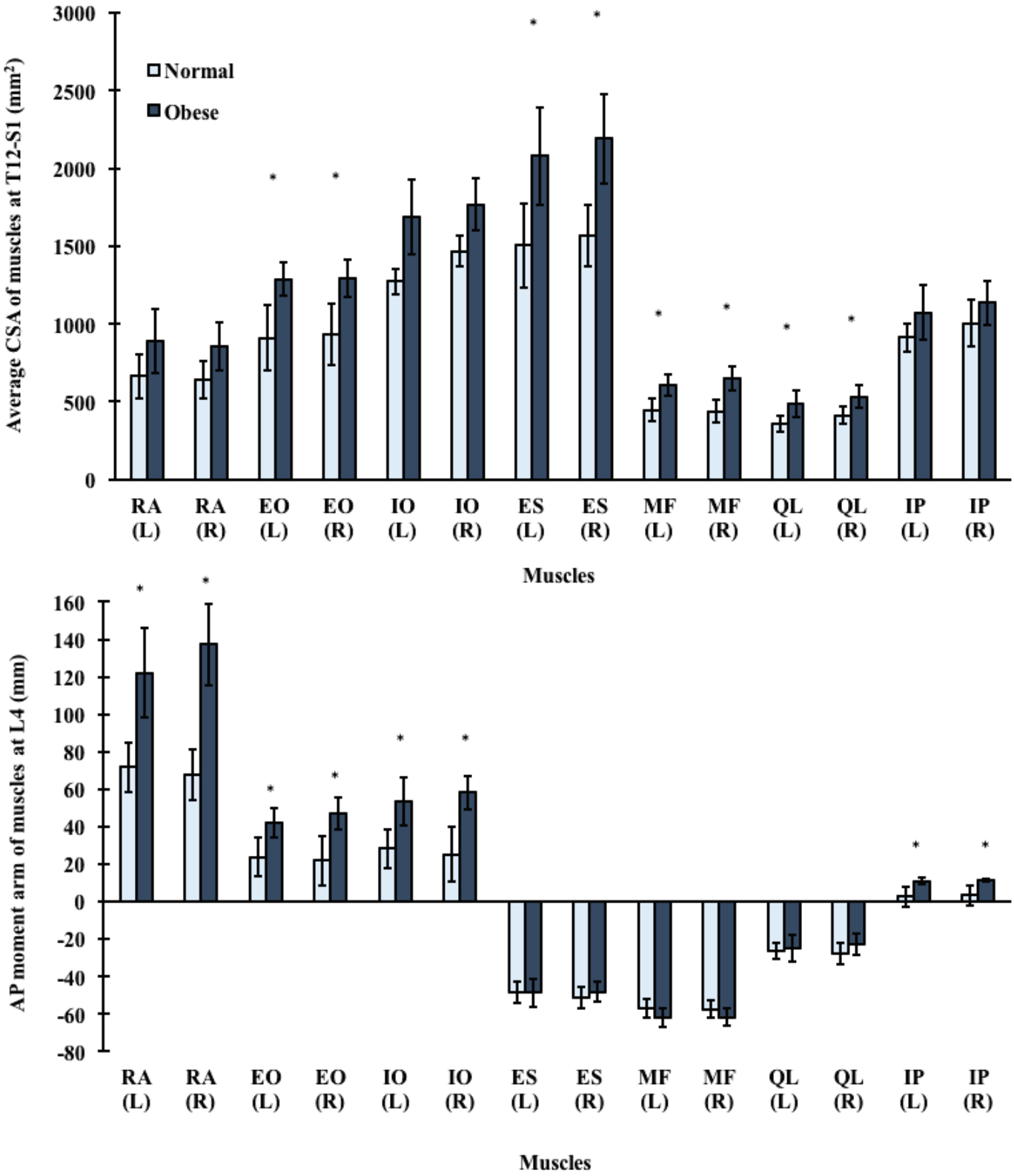

Average CSA of muscles at T12-S1 (mm²)
3000
2500
2000
1500
1000
500
0
Normal
Obese
RA (L)
RA (R)
EO (L)
EO (R)
IO (L)
IO (R)
ES (L)
ES (R)
MF (L)
MF (R)
QL (L)
QL (R)
IP (L)
IP (R)
Muscles
AP moment arm of muscles at L4 (mm)
160
140
120
100
80
60
40
20
0
-20
-40
-60
-80
Muscles

Figure 5

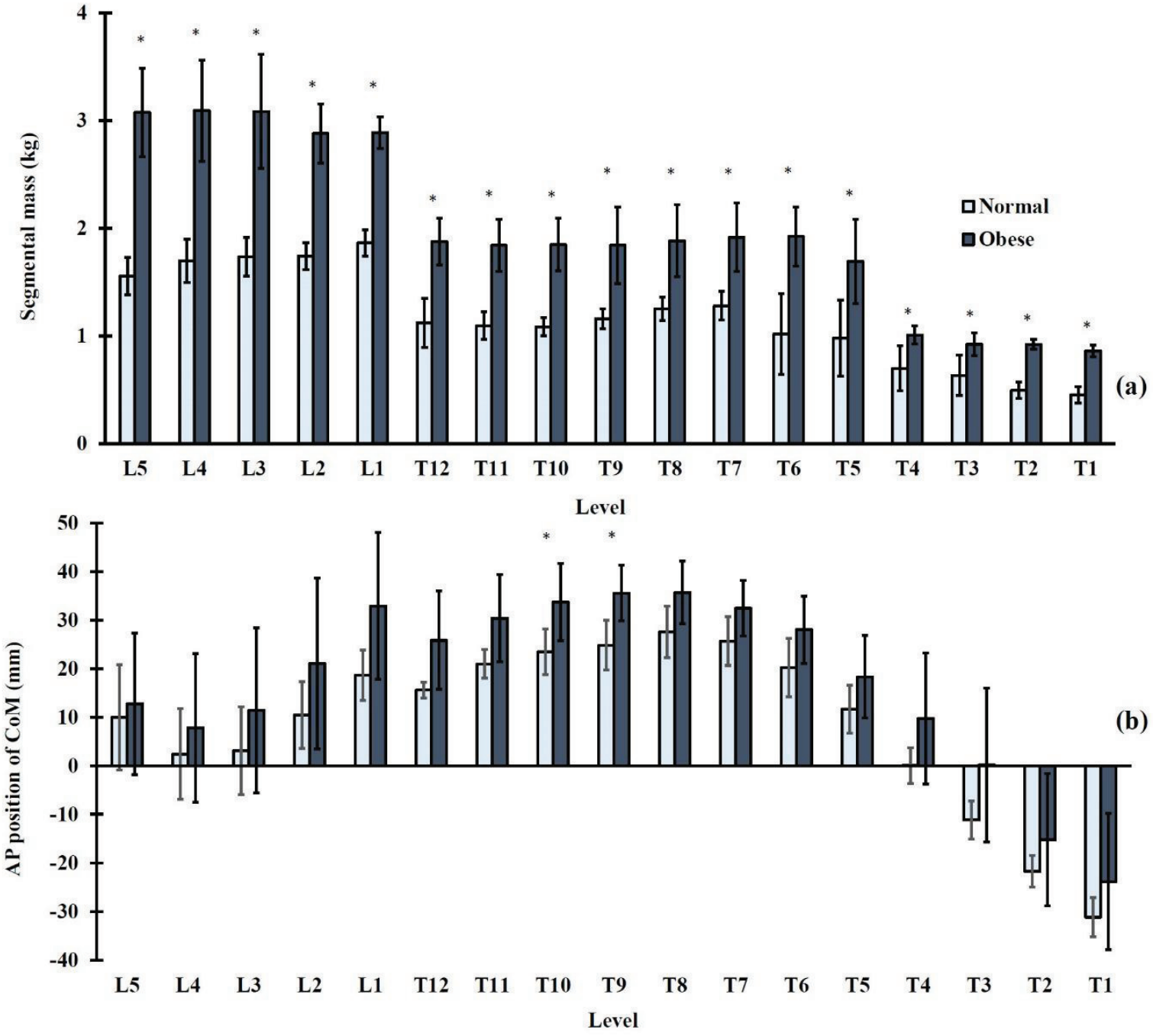

Segmental mass (kg)
4
3
2
1
0
Normal
Obese
(a)
L5 L4 L3 L2 L1 T12 T11 T10 T9 T8 T7 T6 T5 T4 T3 T2 T1
Level
AP position of CoM (mm)
50
40
30
20
10
0
-10
-20
-30
-40
(b)
L5 L4 L3 L2 L1 T12 T11 T10 T9 T8 T7 T6 T5 T4 T3 T2 T1
Level

Figure 6

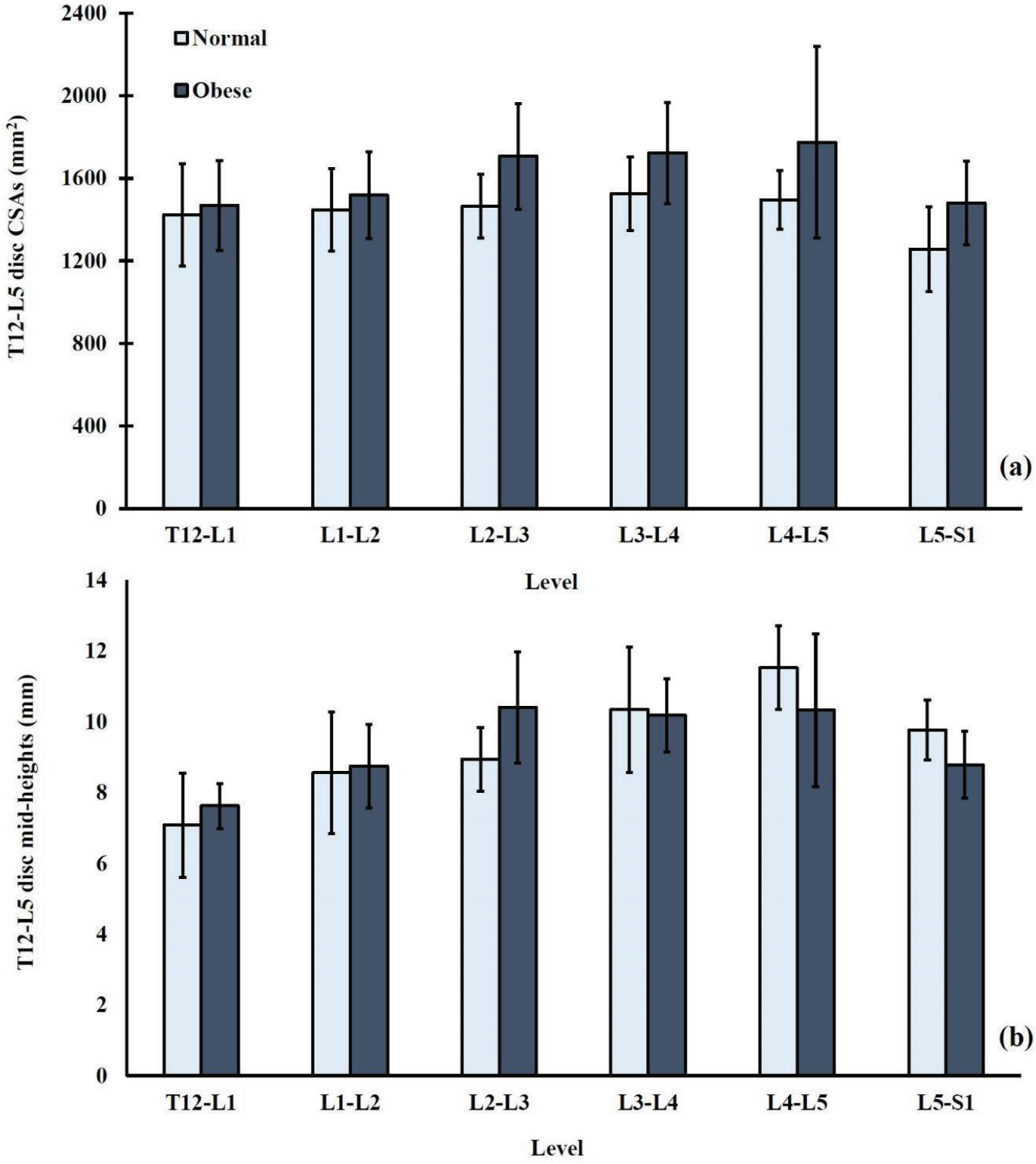

2400
2000
1600
1200
800
400
0
Normal
Obese
T12-L5 disc CSAs (mm²)
(a)
T12-L1
L1-L2
L2-L3
L3-L4
L4-L5
L5-S1
Level
14
12
10
8
6
4
2
0
T12-L5 disc mid-heights (mm)
(b)
T12-L1
L1-L2
L2-L3
L3-L4
L4-L5
L5-S1
Level

Figure 7

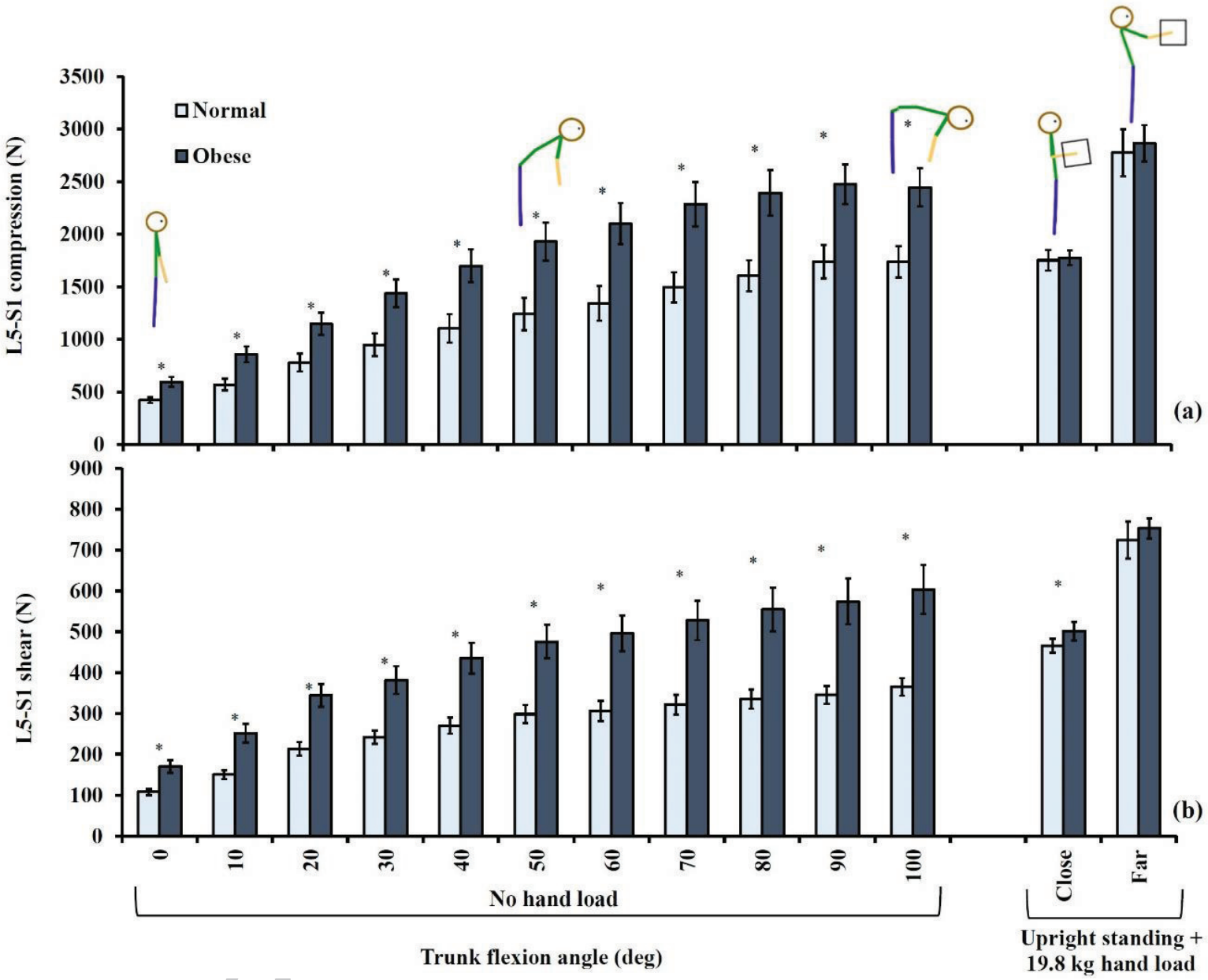

L5-S1 compression (N)
3500
3000
2500
2000
1500
1000
500
0
Normal
Obese
(a)
L5-S1 shear (N)
900
800
700
600
500
400
300
200
100
0
(b)
0
10
20
30
40
50
60
70
80
90
100
Close
Far
No hand load
Trunk flexion angle (deg)
Upright standing +
19.8 kg hand load

Figure 8

ACCEPTED MANUSCRIPT

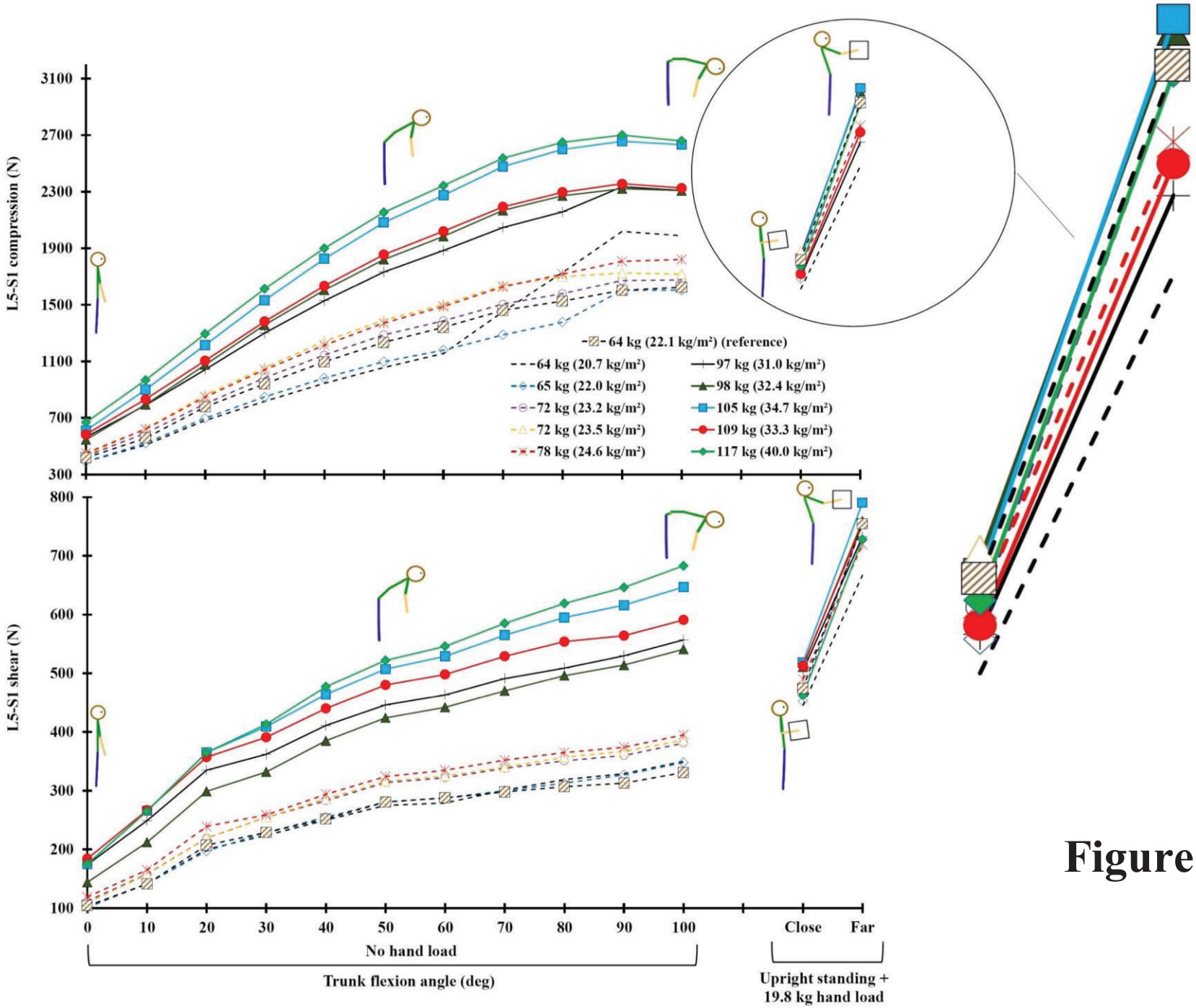


Figure 9

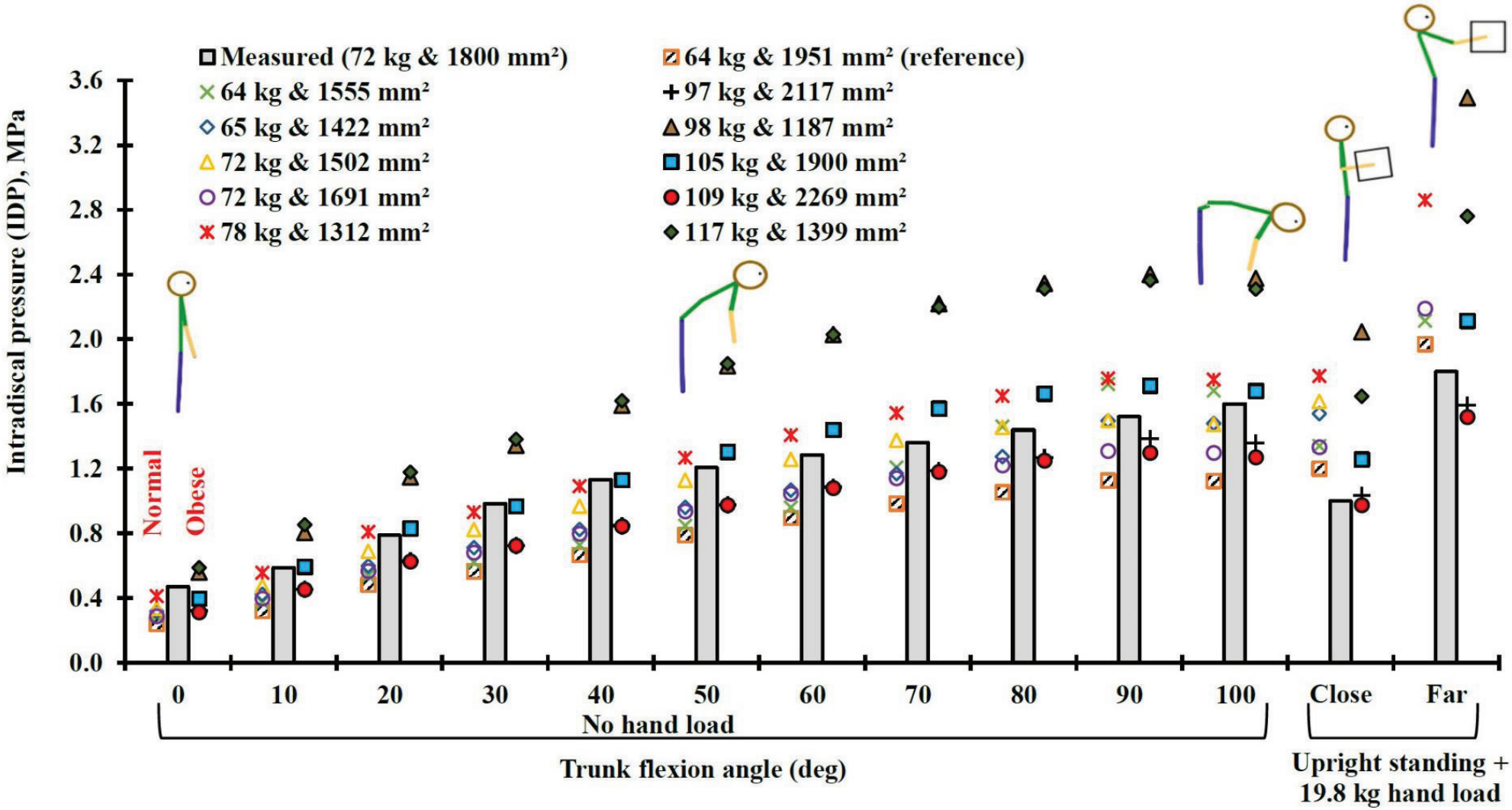

Measured (72 kg & 1800 mm²)
64 kg & 1951 mm² (reference)
64 kg & 1555 mm²
97 kg & 2117 mm²
65 kg & 1422 mm²
98 kg & 1187 mm²
72 kg & 1502 mm²
105 kg & 1900 mm²
72 kg & 1691 mm²
109 kg & 2269 mm²
78 kg & 1312 mm²
117 kg & 1399 mm²
Intradiscal pressure (IDP), MPa
3.6
3.2
2.8
2.4
2.0
1.6
1.2
0.8
0.4
0.0
Normal
Obese
0
10
20
30
40
50
60
70
80
90
100
Close
Far
No hand load
Trunk flexion angle (deg)
Upright standing + 19.8 kg hand load

Figure 10